Biogeosciences, 13, 3777–3791, 2016
www.biogeosciences.net/13/3777/2016/
doi:10.5194/bg-13-3777-2016

Biogeosciences Open Access EGU

Summer fluxes of methane and carbon dioxide from a pond and floating mat in a continental Canadian peatland

Magdalena Burger[1,2], **Sina Berger**[1,2], **Ines Spangenberg**[1,2], **and Christian Blodau**[1,2]

[1]Ecohydrology and Biogeochemistry Group, Institute of Landscape Ecology, University of Münster, Münster, Germany
[2]School of Environmental Sciences, University of Guelph, Guelph, Canada

Correspondence to: Christian Blodau (christian.blodau@uni-muenster.de)

Received: 22 November 2015 – Published in Biogeosciences Discuss.: 22 January 2016
Revised: 14 May 2016 – Accepted: 17 May 2016 – Published: 30 June 2016

Abstract. Ponds smaller than 10 000 m^2 likely account for about one-third of the global lake perimeter. The release of methane (CH_4) and carbon dioxide (CO_2) from these ponds is often high and significant on the landscape scale. We measured CO_2 and CH_4 fluxes in a temperate peatland in southern Ontario, Canada, in summer 2014 along a transect from the open water of a small pond (847 m^2) towards the surrounding floating mat (5993 m^2) and in a peatland reference area. We used a high-frequency closed chamber technique and distinguished between diffusive and ebullitive CH_4 fluxes. CH_4 fluxes and CH_4 bubble frequency increased from a median of 0.14 (0.00 to 0.43) mmol m^{-2} h^{-1} and 4 events m^{-2} h^{-1} on the open water to a median of 0.80 (0.20 to 14.97) mmol m^{-2} h^{-1} and 168 events m^{-2} h^{-1} on the floating mat. The mat was a summer hot spot of CH_4 emissions. Fluxes were 1 order of magnitude higher than at an adjacent peatland site. During daytime the pond was a net source of CO_2 equivalents to the atmosphere amounting to 0.13 (−0.02 to 1.06) g CO_2 equivalents m^{-2} h^{-1}, whereas the adjacent peatland site acted as a sink of −0.78 (−1.54 to 0.29) g CO_2 equivalents m^{-2} h^{-1}. The photosynthetic CO_2 uptake on the floating mat did not counterbalance the high CH_4 emissions, which turned the floating mat into a strong net source of 0.21 (−0.11 to 2.12) g CO_2 equivalents m^{-2} h^{-1}. This study highlights the large small-scale variability of CH_4 fluxes and CH_4 bubble frequency at the peatland–pond interface and the importance of the often large ecotone areas surrounding small ponds as a source of greenhouse gases to the atmosphere.

1 Introduction

Inland waters play a significant role in the global carbon cycle although covering only 3.7 % of the Earth's land surface (Bastviken et al., 2011; Raymond et al., 2013; Tranvik et al., 2009). They transport and sequester autochthonous and terrestrially derived carbon and are also sources of carbon dioxide (CO_2) and methane (CH_4) to the atmosphere (Cole et al., 2007; Tranvik et al., 2009). Global estimates of CO_2 and CH_4 emissions from inland waters have recently been corrected upward to 2.1 Pg C yr^{-1} as CO_2 (Raymond et al., 2013) and 0.65 Pg C yr^{-1} as CH_4 (Bastviken et al., 2011). Together they are similar to the net carbon uptake by terrestrial ecosystems of -2.5 ± 1.3 Pg C yr^{-1} and to approximately one-third of the anthropogenic CO_2 emissions (Ciais et al., 2013).

Small aquatic systems may be particularly important in this respect (Downing, 2010). According to high-resolution satellite imagery analyzed by Verpoorter et al. (2014), 77 % of the total 117 million lakes belong to the smallest detectable size category of 2000 to 10 000 m^2 lake area. These waters only contribute 7 % to the area but 32 % to the total lake perimeter (Verpoorter et al., 2014). Numerous processes were found to proceed faster in small aquatic systems than in larger ones. Sequestration rates of organic carbon (Downing, 2010; Downing et al., 2008), the concentrations of CH_4, CO_2, and dissolved organic carbon (DOC) in the water column (Bastviken et al., 2004; Juutinen et al., 2009; Kelly et al., 2001; Kortelainen et al., 2006; Xenopoulos et al., 2003), and CH_4 and CO_2 emissions from the water to the atmosphere increase with decreasing lake size (Juutinen et al., 2009; Kortelainen et al., 2006; Michmerhuizen et al., 1996; Repo et al., 2007).

Small and shallow lakes and ponds are common in flat northern glacial landscapes and abundant in peatland areas, where 20 to 30 % of the world's soil organic carbon is stored (Turunen et al., 2002). CO_2 emissions from peatland ponds were reported to be in the same order of magnitude than net uptake of CO_2 by the peatland vegetation (Dinsmore et al., 2009; Hamilton et al., 1994). CH_4 emissions from open waters generally exceed CH_4 fluxes from vegetated areas by a factor 3 to 25 (Hamilton et al., 1994; McLaughlin and Webster, 2014; Trudeau et al., 2013). Small and shallow peatland ponds have been generally found to be particular strong emitters of the gas (McEnroe et al., 2009; Trudeau et al., 2013). Moreover, CH_4 and CO_2 emissions from open waters can be significant on the landscape scale despite their often small area (Dinsmore et al., 2010; Juutinen et al., 2013). Pelletier et al. (2014) estimated that a pond cover of > 37 % could convert a northern peatland from a carbon sink into a carbon source. Such findings are relevant as Hamilton et al. (1994) and Trudeau et al. (2013) reported a pond cover of 8 to 12 and 42 % in fens and bogs in northern Canada. The authors suspected a contribution of aquatic CH_4 fluxes to landscape CH_4 fluxes of 30 and 79 %, respectively. Very high CH_4 emissions have also been reported from a floating mat on a thermokarst pond and a floating mat within a bog pond (Flessa et al., 2008; Sugimoto and Fujita, 1997). Juutinen et al. (2013) documented highest CH_4 fluxes from a wet lawn adjacent to a small fen lake compared to the lake itself and fen lawns farther away from the small lake.

Fluxes of CH_4 and CO_2 from ponds are controlled by environmental and biotic factors. Atmospheric CH_4 fluxes are controlled by microbial production and oxidation of CH_4 within peat, sediment and surface water and the diffusive, ebullitive, and plant-mediated transport to the atmosphere (Bastviken et al., 2004; Bridgham et al., 2013; Carmichael et al., 2014). CO_2 exchange is driven by the interplay of heterotrophic and autotrophic respiration and by photosynthesis of aquatic macrophytes and algae. Both gas fluxes are linked to the quantity and quality of organic and inorganic carbon supplied from the surrounding catchment (Huttunen et al., 2002; Macrae et al., 2004; Tranvik et al., 2009). They are also related to temperature, wind speed and air pressure (e. g. Trudeau et al., 2013; Varadharajan and Hemond, 2012; Wik et al., 2013). Ebullition appears to be of particular importance for CH_4 release to the atmosphere (Walter et al., 2006; Wik et al., 2013) and varies on scales of several tens to hundreds of meters (Bastviken et al., 2004; Wik et al., 2013). Emissions of CH_4 are generally lower in the pelagic than in the littoral zone, where plant habitats further influence fluxes (Juutinen et al., 2001; Larmola et al., 2004). On the other hand, Trudeau et al. (2013) found 2.5 to 5 times lower CH_4 fluxes at the border of fen pools than in the center of the pools with areas of 60 and 200 m^2. Measurements in this study were carried out in a situation where pool size has been historically increasing at the expense of surrounding terrestrial areas.

Despite this progress, knowledge on the temporal and spatial variability of CH_4 and CO_2 fluxes within small pond systems is limited. We know, for example, little about the CH_4 and CO_2 exchange of transition zones between ponds and surrounding peatlands, which can be especially important due to the high perimeter to area ratio of small ponds (Verpoorter et al., 2014). It is important to consider the net effect of different microforms of peatlands by taking into account the global warming potentials, as CH_4 emissions may easily offset carbon sinks in ponds. To gain more insight into these issues we investigated the summer atmospheric CO_2 and CH_4 exchange of open water, a floating mat and an adjacent peatland area in a temperate peatland in southern Ontario, Canada. In particular we tested the hypothesis that (i) ebullitive and diffusive CH_4 fluxes increase from the open water towards a floating mat surrounding the pond. We examined further the expectation that (ii) CH_4 and CO_2 effluxes from the system increase with temperature and wind speed, and investigated if falling air pressure raises CH_4 fluxes. To assess the importance of the pond system for the greenhouse gas balance we calculated the net radiative forcing of the investigated peatland microforms.

2 Materials and methods

2.1 Study site

Wylde Lake Bog is located in the southeastern part of the Luther Marsh Wildlife Management Area (43°54.667′ N, 80°24.022′ W) (Fig. 1) at about 490 m above sea level and has an area of approximately 7.8 km^2. A 600 cm deep profile analyzed by Givelet et al. (2003) documented clay-rich sediments up to 560 cm depth, gyttja from 560 to 490 cm, fen peat from 490 to approximately 300 cm and bog peat above 300 cm depth. The peatland is dominated by mosses, graminoids, dwarf shrubs and sporadic trees, and a pronounced hummock-hollow-microtopography. Common in the peatland are *Sphagnum magellanicum*, *S. capillifolium*, *Carex disperma* and *Chamaedaphne calyculata* and on the floating mat *S. angustifolium*, *S. magellanicum* and *Rhynchospora alba*. The plant species composition of the study site is given in the Supplement (Table S1). The vicinity of the pond is characterized by small open and larger treed areas dominated by *Larix laricina* and *Picea mariana*. The pond (Fig. 1) has an area of 847 m^2 and a depth of 0.3 to 0.8 m. The interface between the water column and the organic deposits is not clearly delimited but consists of a transition zone with suspended organic material. It likely has changed in size, depth, and shape throughout the last decades. Sandilands (1984) reported that larger, adjacent Wylde Lake shrunk from 0.4 km^2 in 1928 to 0.05 km^2 in 1984. The floating mat (Fig. 1) surrounding the pond has an area of approx. 5993 m^2. Climate is temperate continental with a mean annual air temperature of about 6.7 °C, annual

precipitation of 946 mm including 148 mm of snowfall, and an average frost-free period from 7 May to 6 October (1981 to 2010, Fergus Shand Dam, National Climate Data and Information Archive, 2014).

2.2 Environmental variables

Air temperature, relative humidity, wind speed, wind direction, photosynthetically active radiation (PAR) and precipitation were recorded at the study site by a HOBO U30 weather station (U30-NRC-SYS-B, Onset) (Table S2). Water temperature of the pond and the temperature of the floating mat were also continuously measured. Air pressure was recorded at a distance of 1.1 km from the study site (Table S2). In addition we qualitatively observed presence of algae in the pond and occasionally took pictures of the pond and algae.

2.3 CH_4 and CO_2 flux measurements with closed chambers

CH_4 and CO_2 fluxes of the pond and the floating mat were measured once a week from 10 July to 29 September 2014 between 1 p.m. ± 1.5 h and 5 p.m. ± 1.5 h using closed chambers designed according to Drösler (2005). We used a long wooden board floating on air-filled canisters on the pond-end ("floating boardwalk") to do our measurements and to minimize pressure on the ground (Supplement Fig. S1). The other end was secured at the drier end of the floating mat. The cylindrical, transparent Plexiglas chambers had a basal area of 0.12 m^2 and a height of 0.40 m. They were equipped with two or three fans (Micronel Ventilator D341T012GK-2, BEDEK GmbH) to circulate the air, a photosynthetically active radiation (Photosynthetic Light (PAR) Smart Sensor, S-LIA-M002, Onset) and an air temperature sensor (RH Smart Sensor, S-THB-M002, Onset; see also Supplement for further information on instrumentation, Table S2). To compensate for air pressure differences, we attached a vent tube, 12 cm long and 7 mm inner diameter, to the chamber (Davidson et al., 2002). Transparent chambers were used to measure net ecosystem exchange (NEE) and cooled with up to six ice packs depending on ambient temperature to ensure a temperature change of less than 1 °C during the chamber closure. For the measurements, chamber orientation was adjusted to avoid shading of the chamber basal area by the ice packs. Ecosystem respiration (ER) was measured with chambers covered with reflective insolation foil. On the water, chambers were operated with a Styrofoam float (0.80 m × 0.61 m × 0.08 m). The chamber walls extended 10 cm below the water surface as recommended by Soumis et al. (2008). CH_4 and CO_2 concentrations were quantified with an Ultraportable Greenhouse Gas Analyzer (915-001, Los Gatos Research) at a temporal resolution of 1 s. According to the manufacturer, a single data point has a precision of < 2 ppb for CH_4 and < 300 ppb for CO_2. Stability of the calibration was checked in March and August 2014.

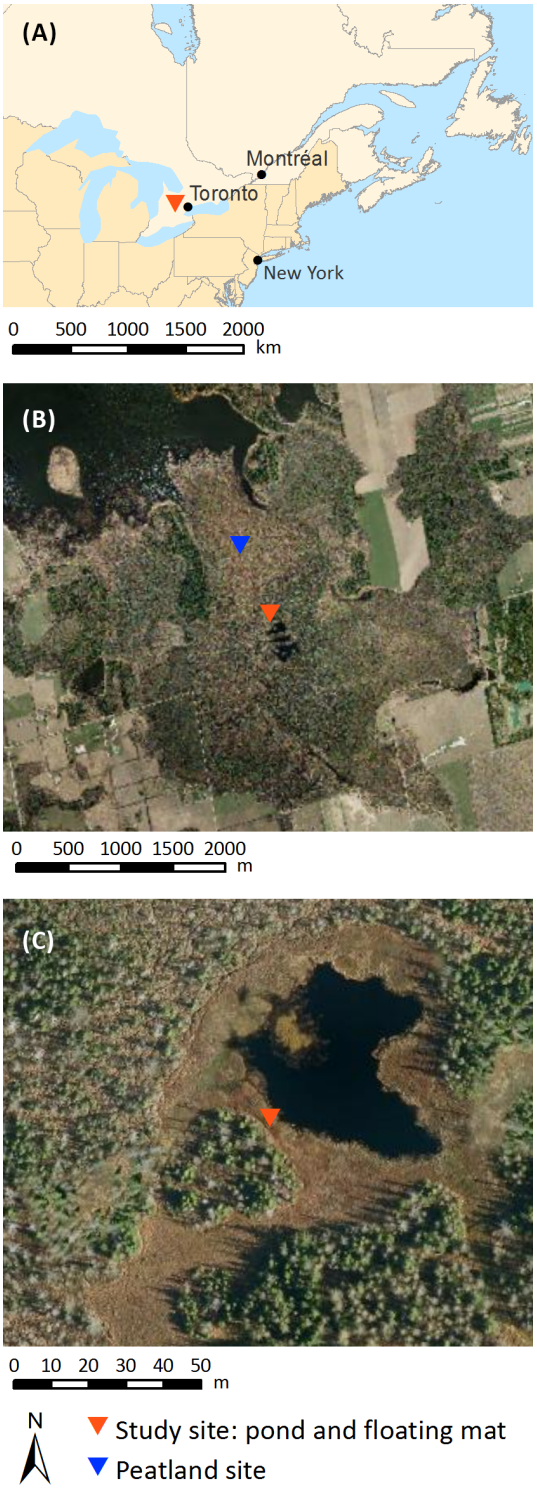

Figure 1. Location of the study site in southern Ontario, Canada **(a)**, studied pond with floating mat and peatland site in Wylde Lake Bog in the Luther Marsh Wildlife Management Area with Luther Lake in the northwest **(b)** and close-up of the studied pond and floating mat **(c)** (Grand River Conservation Authority, 2015).

The air was circulated between the chamber and the analyzer through low-density polyethylene tubes of 5 m length with an inner diameter of 2 mm and a water vapor trap. Using this setup it took 36 s until the sampling cell of the analyzer was fully flushed and the concentration had stabilized.

Flux measurements on the open water were carried out in six locations with increasing distance of 0.7 to 4.6 m to the floating mat (Supplement Table S3). A float with chamber was secured in place by a couple of telescopic poles that were rigidly connected to the floating boardwalk. This way we avoided a drifting of the chamber. On the floating mat the chambers were placed on cylindrical PVC collars with a height of 25 cm. Collars had been inserted into the mat to depths of approximately 15 cm prior to the first measurement. Each sampling day, fluxes were measured at least once with the transparent and with the radiation-shielded chamber, for 5 min on the pond and 3 min on the floating mat, by placing the chamber gently as soon as the concentration reading was stable. When CH_4 concentrations increased sharply within the first 60 s of the measurement due to CH_4 bubble release caused by the positioning of the chamber, the measurement was discarded and repeated. Fluxes were also quantified at a peatland site in the north–northeast of the pond (Fig. 1) with the same approach, every other week from 4 July until 1 October 2014, on 12 measuring plots covering hummocks, hollows, and lawns. In this area of the peatland, hummocks cover 90 % of the area, hollows 9.8 % and lawns 0.2 % of the area.

Fluxes were calculated based on the gas concentration change in the chamber over time using linear regression and the ideal gas law, mean air temperature inside the chamber and the corresponding half hour mean air pressure. The chamber volume was calculated for each measurement depending on the number of ice packs, immersion depth on the pond and mean vegetation height on the floating mat. The first 40 s after chamber deployment were discarded for flux calculation due to the response time of the concentration measurement. If the slope was not significantly different from 0 (F test, $\alpha = 0.05$), the flux was set to 0. Concentration change over time was only < 3 ppm CO_2 and < 0.1 ppm CH_4 in 12 % of flux measurements. These measurements resulted in fluxes close to 0 with $R^2 < 0.8$. Following Repo et al. (2007), we included them in the data set because their exclusion would have biased the results by increasing the median diffusive fluxes by 52 % (CO_2) and 12 % (CH_4).

Due to the high temporal resolution of concentration measurements, we were able to quantify CH_4 fluxes with and without bubbles. When the CH_4 concentrations evolved linearly with a constant slope we used linear regression over the entire time of sampling; when the initial concentration trend was interrupted by one or several sharp increases in slope, followed by a return to the initial slope (Fig. S1), we used piecewise linear fitting for each of the linear segments (Goodrich et al., 2011). According to Goodrich et al. (2011) and Xiao et al. (2014), we define sharp increases in slope as ebullitive CH_4 fluxes and all others as diffusive or continuous flux of micro-bubbles. Time-weighted averages including diffusive and ebullitive flux segments were calculated. We also computed the CH_4 bubble frequency in events $m^{-2}\,h^{-1}$ as the number of bubble events divided by measuring time and area. In order to evaluate the contribution of ebullitive CH_4 flux to the total CH_4 flux, the CH_4 release of each event in µmol was calculated by multiplying the ebullitive flux with the duration of the event and the basal area of the chamber.

For comparisons of NEE between sites and with time, we used the maximum NEE defined as light-saturated at PAR levels > 1000 µmol $m^{-2}\,s^{-1}$ according to a study by Larmola et al. (2013). We further calculated the net exchange of CO_2 equivalents for each flux measurement. To this end, the CH_4 flux was converted into CO_2 equivalents by multiplying the mass flux with the global warming potential of 28 for a 100 year time horizon (Myhre et al., 2013). Subsequently, the CH_4 flux in CO_2 equivalents and the maximum NEE were summed up.

2.4 CO_2 concentration measurements and gradient flux calculations

To obtain estimates of daily time series of CO_2 concentration and fluxes, concentrations of CO_2 in the surface water of the pond and in the air were measured with calibrated non-dispersive infrared absorption sensors (CARBOCAB, GMP222, Vaisala) in the range up to 10 000 ppm and with an accuracy of $\pm$ 150 ppm plus 2 % of the reading. The probe was enclosed in CO_2 permeable silicone tubes, as already used by Estop-Aragonés et al. (2012) in peats, and attached to a floating platform at a depth of approximately 18 cm and a distance of 3.2 m from the pond margin. In water equilibration time to 90 % of dissolved concentration was approximately 1 h when concentration increased but more delayed when it fell (Fig. S3). The platform also carried the data logger (MI70, Vaisala). Another silicon-covered sensor measured air CO_2 concentrations at 0.3 m above the water surface. Concentration was recorded every 15 min and CO_2 flux across the air–water interface estimated according to the boundary layer equation approach (Supplement). Due to frequent failures of the sensors with increased humidity in the sensor head and overheating of the data logger, CO_2 fluxes were only calculated for 5 and 3 exemplary days in July and September, respectively. During these periods sensor functioning was stable.

2.5 CH_4 and CO_2 concentrations and diffusive fluxes in the sediment

Dissolved CH_4 and CO_2 concentrations at the sediment–water interface were determined with pore water peepers of 60 cm length and 1 cm resolution as developed by

Hesslein (1976). The chambers were filled with deionized water, covered with a nylon membrane of 0.2 µm pore size, installed at four locations randomly distributed across the pond on 21 August 2014 and sampled on 25 and 29 September 2014. The pH of every other cell was measured in the field and a sample of 0.5 mL from each chamber filled into a vial containing 20 µL of 4 M hydrochloric acid (HCl). CO_2 and CH_4 concentrations in the headspace of the vials were determined with an SRI 8610C gas chromatograph equipped with a methanizer and a flame ionization detector on the day after sampling. The original CO_2 and CH_4 concentrations in the pore water were calculated by using the measured headspace concentrations, Henry's law with temperature corrected Henry's law constants (Sander, 1999) and the ideal gas law. Diffusive fluxes of CO_2 and CH_4 towards the sediment–water interface were calculated with Fick's first law and diffusion coefficients in water D_w corrected for an assumed sediment temperature of 15 °C (CH_4: 1.67×10^{-5} cm^2 s^{-1}; CO_2: 1.87×10^{-5} cm^2 s^{-1}) and assuming a porosity n of 0.9. The effect of porosity on the sediment diffusion coefficient was accounted for by multiplying D_w with a factor n^2 (Lerman, 1978). We further calculated a theoretical temperature- and depth-dependent threshold of bubble formation using Henry's law, correcting Henry's law constant for a temperature of 15 °C, and assuming a partial pressure of N_2 in the pore water of 0.8 or 0.5 atm. The assumption here is that bubble formation is possible when the partial pressure of CH_4 and remaining N_2 exceeds atmospheric and water pressure in the anoxic sediment. In addition we sampled occasionally gas bubbles trapped in an algal mat that was present on the pond until 12 August.

2.6 Statistical analyses

Statistical analyses were performed with R, version 3.1.2 (R Core Team, 2014). All data sets were checked for normality with the Shapiro–Wilk normality test at a confidence level of $\alpha = 0.05$. To investigate statistical differences of a continuous variable between two or more groups, we used the non-parametric Kruskal–Wallis rank sum test ($\alpha = 0.05$) and if applicable afterwards the multiple comparison test after Kruskal–Wallis ($\alpha = 0.05$) since none of the data sets were normally distributed. For the investigation of relationships between two continuous variables, we used Spearman's rank correlation ($\alpha = 0.05$). Due to visually different dynamics of the gas fluxes from 10 July to 7 August (here called "mid summer") compared to 15 August to 29 September (here called "late summer"), correlations with environmental variables were examined for the whole period as well as the two subperiods.

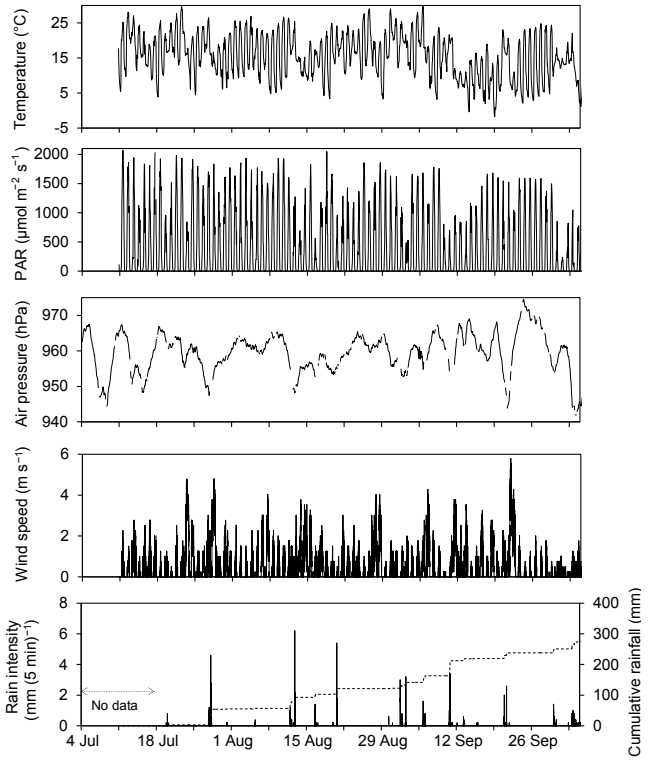

Figure 2. Time series of weather variables at the study site. Air temperature, photosynthetically active radiation (PAR) and air pressure are shown as hourly means, wind speed and rain intensity as 5 min averages. The dashed line in the lowest panel shows the cumulative rainfall.

3 Results

3.1 Weather and pond conditions

Three distinct periods of weather occurred. From 10 July until 10 September 2014, air temperatures remained high with a mean (±standard deviation) of 17.0 ± 2.7 °C (Fig. 2). Most days were sunny with some passing clouds. From 11 to 22 September 2014, mean air temperature had cooled to 10.2 ± 2.8 °C and the first frost occurred on 14 September (Fig. 2). From 23 to 29 September, mean air temperature was 13.2 ± 7.6 °C with a high daily amplitude from 3.7 ± 1.3 to 24.3 ± 1.5 °C and wind speed was low with a mean of 0.14 ± 0.31 m s^{-1} (Fig. 2). Major storms with maximum wind speeds from 3 to 5.5 m s^{-1} on 23 and 28 July, 12 August, 6, 11 and 21 September were accompanied by air pressure decline to lows between 944 and 955 hPa. Often rainfall reached an intensity of 2.8 to 6.2 mm in the chosen 5 min time intervals (Fig. 2).

During the summer an algae mat developed in the pond that impeded water circulation (see Supplement for visuals). This algae mat was irreversibly dissolved with the storm on 12 August. As gas exchange with the atmosphere distinctly

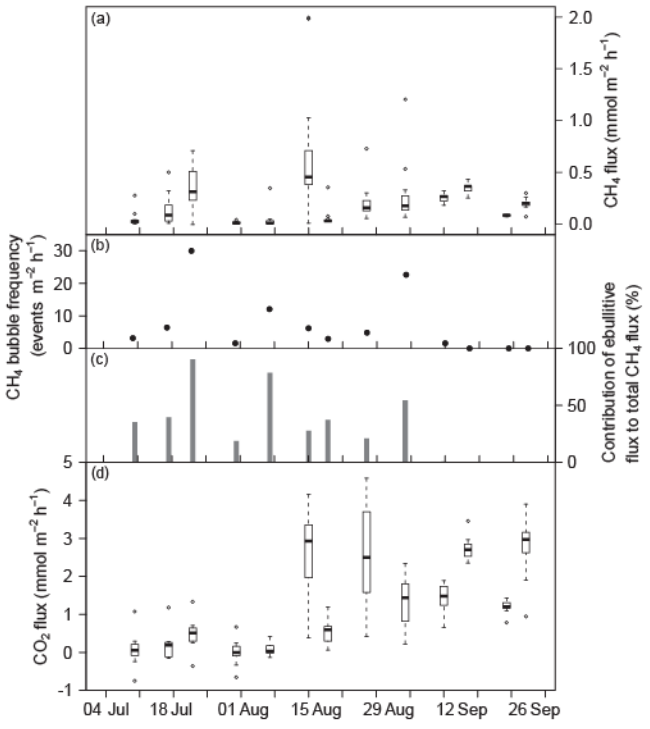

Figure 3. Time series of pond CH_4 fluxes (**a**), CH_4 bubble frequency (**b**), contribution of ebullitive CH_4 flux to total CH_4 flux (**c**) and CO_2 fluxes (**d**) on measuring days from 10 July until 29 September 2014. In panels (**a**) and (**d**), the bold horizontal line shows the median, the bottom and the top of the box the 25 and 75 percentile and the whiskers include all values within 1.5 times the interquartile range.

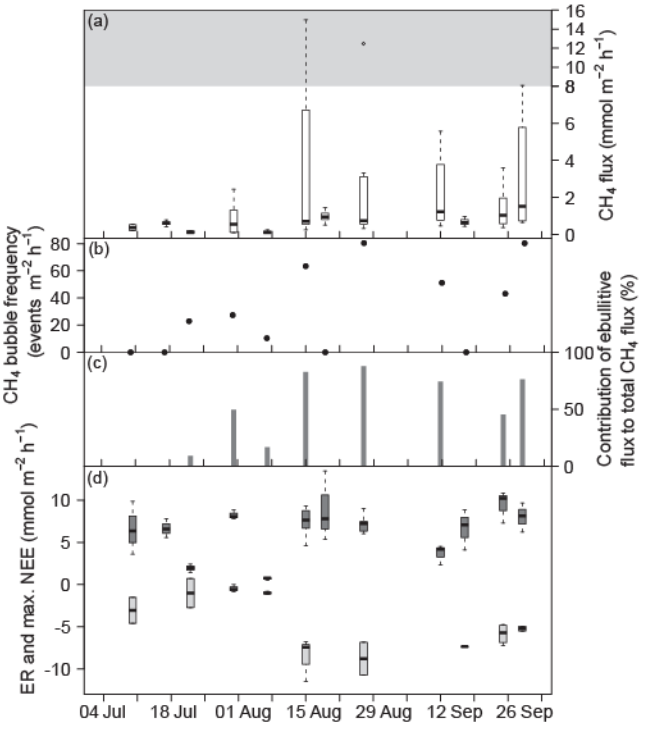

Figure 4. Time series of floating mat CH_4 fluxes (**a**), CH_4 bubble frequency (**b**), contribution of ebullitive CH_4 flux to total CH_4 flux (**c**) as well as ecosystem respiration (ER) and maximum net ecosystem exchange (NEE) (**d**) on measuring days from 10 July until 29 September 2014. Note the different scaling of the y axis within the gray area in panel (**a**). In panel (**d**), the dark gray boxes show the daytime ER and the light gray boxes the maximum net ecosystem exchange at values of photosynthetically active radiation $> 1000\,\mu mol\,m^{-2}\,s^{-1}$. In panels (**a**) and (**d**), the bold horizontal line shows the median, the bottom and the top of the box the 25 and 75 percentile and the whiskers include all values within 1.5 times the interquartile range.

differed before and after this event, we used the storm as a distinction between "mid summer" and "late summer" conditions throughout the analysis.

3.2 CH_4 and CO_2 fluxes over time

CH_4 fluxes from the pond were significantly lower in the period from 10 July until 7 August with a median of $0.03\,mmol\,m^{-2}\,h^{-1}$ compared to a median of $0.21\,mmol\,m^{-2}\,h^{-1}$ from 15 August until 29 September (Kruskal–Wallis test, $p < 0.001$, $n = 159$) (Fig. 3a). The highest median CH_4 flux, highest maximum flux, and largest variability were observed on 15 August, after the algal mat had been dissolved on 12 August. The bubble frequency varied between 0 and 30 events $m^{-2}\,h^{-1}$ (Fig. 3b) and the contribution of the ebullitive to the total CH_4 flux between 90 % in mid-July and 0 % in late September (Fig. 3c). Efflux of CH_4 from the floating mat was variable but significantly higher in late summer with a median of $0.80\,mmol\,m^{-2}\,h^{-1}$ than in mid summer with a median of $0.22\,mmol\,m^{-2}\,h^{-1}$ (Kruskal–Wallis test, $p < 0.001$, $n = 84$) (Fig. 4a). The bubble frequency on the floating mat ranged from 0 to 80 events $m^{-2}\,h^{-1}$ and the contribution of ebullition to CH_4 flux from 0 to 88 % (Fig. 4b and c). At the peatland site, CH_4 fluxes were similar over time with a median of $0.31\,mmol\,m^{-2}\,h^{-1}$ and two very high individual fluxes in September and October (Fig. 5a). The bubble frequency and contribution of ebullition to CH_4 flux ranged from 0 to 5 events $m^{-2}\,h^{-1}$ and 0 to 54 %, respectively (Fig. 5b and c).

CO_2 fluxes from the pond in mid summer had a median of $0.11\,mmol\,m^{-2}\,h^{-1}$ and were also significantly lower than the pond CO_2 fluxes in late summer with a median of $1.80\,mmol\,m^{-2}\,h^{-1}$ (Kruskal–Wallis test, $p < 0.001$, $n = 159$) (Fig. 3d). During 24 out of 55 individual measurements before 15 August, CO_2 exchange across the water–atmosphere interface was absent or CO_2 was taken up by the pond between 0 and $-0.75\,mmol\,m^{-2}\,h^{-1}$. Subsequently CO_2 was net emitted. The median daytime ER of the floating mat was $6.77\,mmol\,m^{-2}\,h^{-1}$ and the median of the maximum NEE $-4.81\,mmol\,m^{-2}\,h^{-1}$ (Fig. 4d). Daytime ER at the peatland site varied between 2.61 to $36.93\,mmol\,m^{-2}\,h^{-1}$

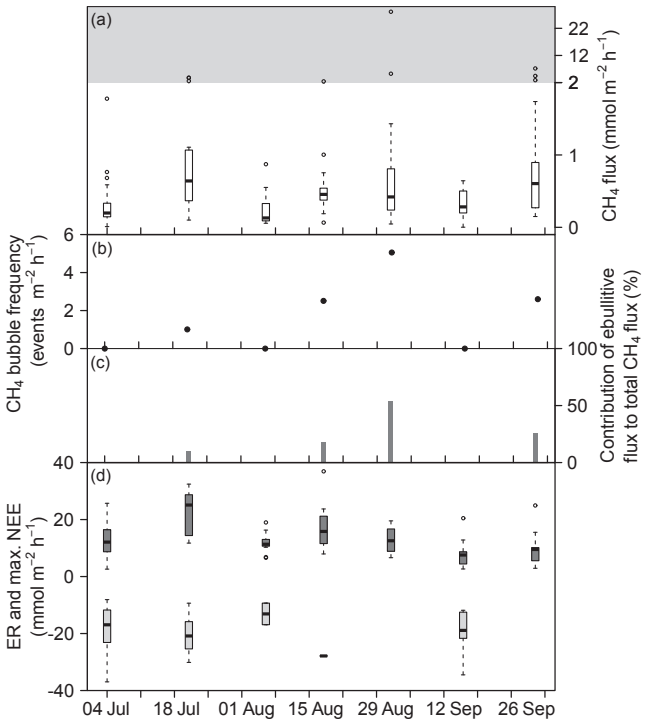

Figure 5. Time series of peatland CH_4 fluxes **(a)**, CH_4 bubble frequency **(b)**, contribution of ebullitive CH_4 flux to total CH_4 flux **(c)** as well as ecosystem respiration (ER) and maximum net ecosystem exchange (NEE) **(d)** on measuring days from 4 July until 1 October 2014. Note the different scaling of the y axis within the gray area in panel **(a)**. In panel **(d)**, the dark gray boxes show the daytime ER and the light gray boxes the maximum net ecosystem exchange at values of photosynthetically active radiation > 1000 µmol m^{-2} s^{-1}. In panels **(a)** and **(d)**, the bold horizontal line shows the median, the bottom and the top of the box the 25 and 75 percentile and the whiskers include all values within 1.5 times the interquartile range.

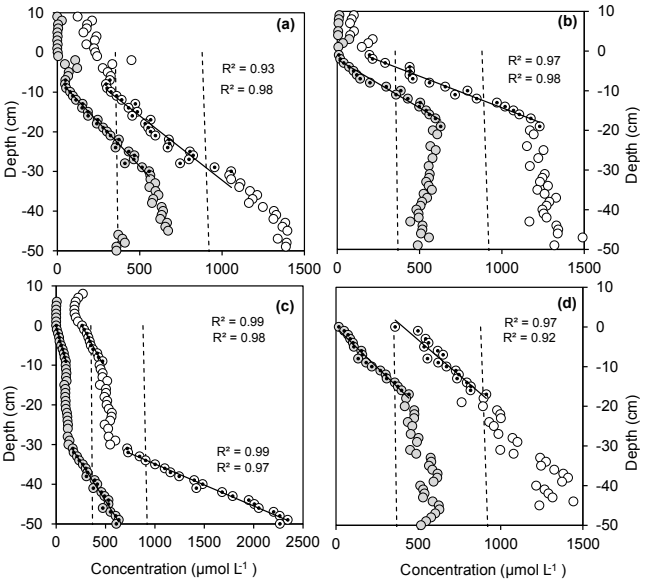

Figure 6. CH_4 (shaded symbols) and CO_2 (open symbols) concentrations near the sediment–water interface and in the sediment of the pond in four locations **(a–d)** on 25 and 29 September respectively, as obtained with porewater peepers. Water depth at the locations was about 0.5 m; a depth of zero on the y axis indicates the assumed sediment–water interface. Black lines represent regression slopes (with regression coefficient R^2) used to calculate diffusive fluxes towards the sediment–water interface. Dashed lines denote depth and temperature dependent theoretical thresholds for formation of CH_4 bubbles at 0.8 atm (lower line) and 0.5 atm (upper line) partial pressure of N_2 in the pond sediment at 15 °C. In panel **(c)** also the diffusive flow from deeper sediment layers was calculated.

with a median of 11.98 mmol m^{-2} h^{-1} and tended to decrease towards fall (Fig. 5d). The maximum NEE was quite constant from July until September with a median of −16.98 mmol m^{-2} h^{-1}.

The gradient method provided similar CO_2 fluxes in July and September with a median of 1.99 mmol m^{-2} h^{-1} in July and 2.02 mmol m^{-2} h^{-1} in September (Fig. S2). The daily amplitude of fluxes determined with this method was 1.46 to 3.19 mmol m^{-2} h^{-1} in July and 1.41 to 1.86 mmol m^{-2} h^{-1} in September (Fig. S2). Comparing results of floating chamber and gradient method, in July, when the algal mat on the pond was present, the daytime CO_2 fluxes obtained by the gradient method were 14-fold higher than the respective CO_2 fluxes measured with the floating chambers (Kruskal–Wallis test, $p < 0.001$, $n = 189$). In September the results of gradient and chamber method were not significantly different.

3.3 CO_2 and CH_4 concentrations and diffusion in the surface water and sediments

CO_2 concentrations of the surface water of the pond were similar during the examined periods in July and September with a mean (±standard deviation) of 114.8 ± 33.1 and 132.0 ± 21.0 µmol L^{-1}, respectively (Fig. S2). In both periods we observed diurnal cycles of CO_2 concentrations covering a mean amplitude of 83.5 ± 16.3 µmol L^{-1} (July) and 62.0 ± 3.1 µmol L^{-1} (September). In the sediments, the mean pH was 4.29 ± 0.11 above the sediment–water interface and increased to 5.37 ± 0.28 at a sediment depth of 40 to 60 cm. CH_4 concentrations rose with depth from an average of 10.7 ± 20.4 µmol L^{-1} above the sediment–water interface to 557.3 ± 72.9 µmol L^{-1} at a depth of 40 to 60 cm into the sediment (Fig. 6). The concentration began exceeding theoretical thresholds for bubble formation at depths between 10 to 40 cm and at a partial pressure of N_2 of 0.8 atm, but nowhere were concentrations sufficient to form bubbles at 0.5 atm N_2 (Fig. 6). The average CO_2 concentration at 40 to 60 cm depth was 1548.2 ± 332.5 µmol L^{-1} and 1 order of magnitude higher than above the sediment–water interface (Fig. 6). Diffusive fluxes towards the surface

water were on average $10.5 \pm 5.6\,\mu mol\,m^{-2}\,h^{-1}$ (CH_4) and $16.9 \pm 9.4\,\mu mol\,m^{-2}\,h^{-1}$ (CO_2), or $12.0 \pm 5.6\,\mu mol\,m^{-2}\,h^{-1}$ (CH_4) and $25.8 \pm 16.1\,\mu mol\,m^{-2}\,h^{-1}$, depending on where the concentration gradient of pore water peeper C is assigned (Fig. 6). In situ production and diffusion from the sediment thus contributed only a small fraction to the CO_2 and CH_4 flux from the pond. The relative inactivity of the pond sediment was also indicated by the mostly flat and linear concentration increase of both gases with depth near the sediment–water interface.

3.4 Spatial pattern of CH_4 and CO_2 fluxes

Efflux of CH_4 increased 6-fold from open water towards the floating mat and was also much higher on the floating mat than at the peatland site (Fig. 7a). The open water median CH_4 flux of plot p1, p2 and p3, farthest away from the floating mat, was $0.12\,mmol\,m^{-2}\,h^{-1}$ and significantly lower than from plot p4, p5 and p6 closer to the floating mat with a median of $0.19\,mmol\,m^{-2}\,h^{-1}$ (Kruskal–Wallis test, $p < 0.05$, $n = 82$) (Table S3). The median CH_4 flux of the floating mat was $0.64\,mmol\,m^{-2}\,h^{-1}$ and significantly higher than the CH_4 flux from the pond (Kruskal–Wallis test, $p < 0.001$, $n = 243$). We observed an increasing frequency of ebullition and a higher contribution to CH_4 flux towards the floating mat. On plot p1 only 4 events $m^{-2}\,h^{-1}$ contributing 5 % occurred, whereas on plot m3 on the floating mat 168 events $m^{-2}\,h^{-1}$ contributing 78 % were found (Fig. 7b and c). The CH_4 flux of m3 was significantly higher than that of m1 and m2 (Kruskal–Wallis multiple comparison test, $p < 0.05$, $n = 84$).

The frequency of ebullition and the amount of CH_4 released by bubble events differed along the transect and in comparison to the peatland site. On the pond, bubble events with a comparatively small CH_4 release of 0 to 2.5 µmol were most frequent and occurred 5.4 times $m^{-2}\,h^{-1}$ (Fig. 8). They also contributed the most to the total CH_4 release. Bubble events releasing a larger amount of CH_4 were rare. The contribution of ebullition to CH_4 release was 27 %. On the floating mat, CH_4 release by individual bubble events was highly variable with a maximum of 50 µmol (Fig. 8). Larger bubble events were less frequent than smaller ones. However, medium and larger bubble events contributed most to CH_4 release with up to 8 %. The contribution of ebullition to CH_4 release was 66 % on the floating mat. In contrast, it was only 20 % in the peatland with a clearly different frequency distribution (Fig. 8). Bubble events occurred over a larger range of release strength than on the pond, but they were less frequent with a total bubble frequency of only 1.3 events $m^{-2}\,h^{-1}$.

The pond was on average also a net source of CO_2 with a median CO_2 efflux of $1.16\,mmol\,m^{-2}\,h^{-1}$ (Fig. 7d). On the floating mat, daytime ER ranged from 0.53 to $13.45\,mmol\,m^{-2}\,h^{-1}$ and maximum NEE from -11.46 to $0.71\,mmol\,m^{-2}\,h^{-1}$ (Fig. 7d).

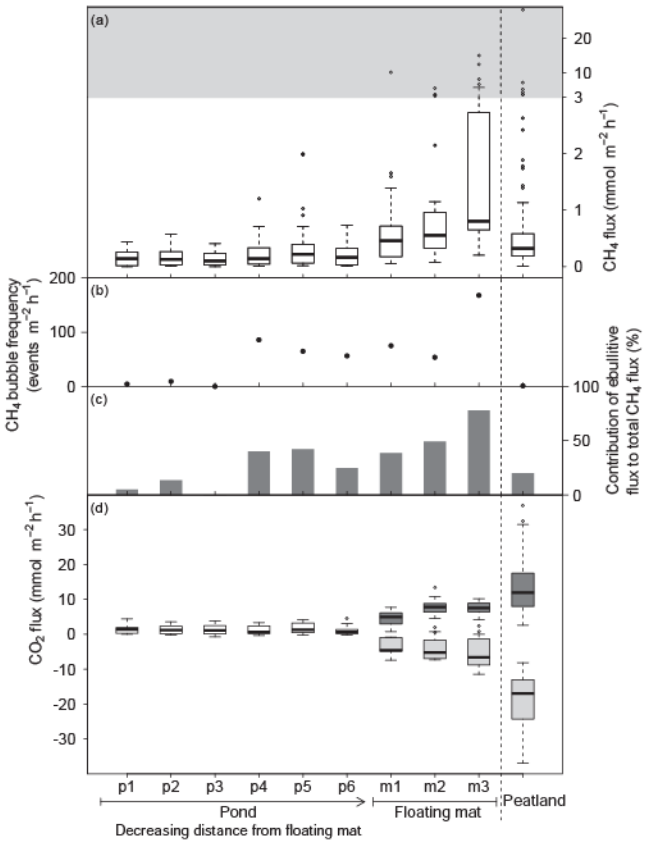

Figure 7. CH_4 fluxes (**a**), CH_4 bubble frequency (**b**), contribution of ebullitive CH_4 flux to total CH_4 flux (**c**) and CO_2 fluxes (**d**) of the pond (p1 to p6) along a gradient of decreasing distance from the floating mat, of the three measuring plots on the floating mat (m1 to m3) and of the peatland site for comparison. Note the different scaling of the *y* axis within the gray area in panel (**a**). In panel (**d**), the transparent boxes show the net CO_2 flux of the pond, the dark gray boxes the daytime ER and the light gray boxes the maximum net ecosystem exchange of the floating mat and the peatland at values of photosynthetically active radiation > $1000\,\mu mol\,m^{-2}\,s^{-1}$. In panels (**a**) and (**d**), the bold horizontal line shows the median, the bottom and the top of the box the 25th and 75th percentile and the whiskers include all values within 1.5 times the interquartile range.

3.5 Controls on CH_4 and CO_2 fluxes

CH_4 and CO_2 fluxes from the pond and ER on the floating mat were significantly negatively, and maximum NEE on the floating mat positively correlated with air, water and mat temperature (Tables 1 and 2). We found more negative NEE values at an increasing PAR on the floating mat as well as on the pond. Late summer fluxes of CO_2 and CH_4 across the water–atmosphere interface were positively correlated with wind speed, whereas the respective mid summer fluxes were negatively correlated (Tables 1 and 2).

Total CH_4 fluxes from the floating mat and the pond were significantly higher for periods with a decreasing air pressure trend over the last 24 h than for periods with an increasing air

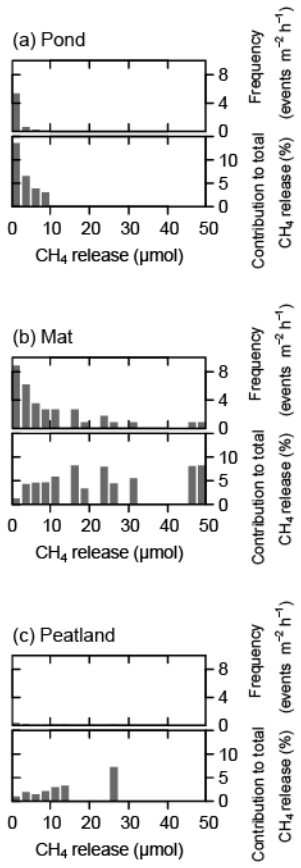

Figure 8. Frequency distribution of ebullitive CH_4 release (upper panels) as well as contribution of each size group of ebullitive CH_4 release to the total CH_4 release (lower panels) of the pond (**a**), the floating mat (**b**) and the peatland (**c**).

pressure trend (Kruskal–Wallis test, $p < 0.05$ and $p < 0.01$, $n = 111$ and $n = 61$). At the floating mat, median fluxes during these periods were 0.82 and 0.55 mmol m^{-2} h^{-1}, on the pond 0.13 and and 0.04 mmol m^{-2} h^{-1} (see also Fig. S4).

3.6 Greenhouse gas exchange of the pond system compared to the surrounding peatland

During our daytime measurements the pond and the floating mat were most frequently significant net sources of CO_2 equivalents, whereas the peatland was generally a sink of CO_2 equivalents (Fig. 9; Kruskal–Wallis multiple comparison test, $p < 0.001$, $n = 218$). The source strength of CO_2 equivalents was largest on the floating mat with a median of 0.21 g CO_2 equivalents m^{-2} h^{-1}. While the floating mat and peatland site took up CO_2 at PAR > 1000 µmol m^{-2} s^{-1}, the pond emitted CO_2 to the atmosphere during 90 % of measurements (see Figs. 3, 4, 5). When both greenhouse gases were emitted, CH_4 contributed 59 ± 20 % to the total emission of CO_2 equivalents of the pond.

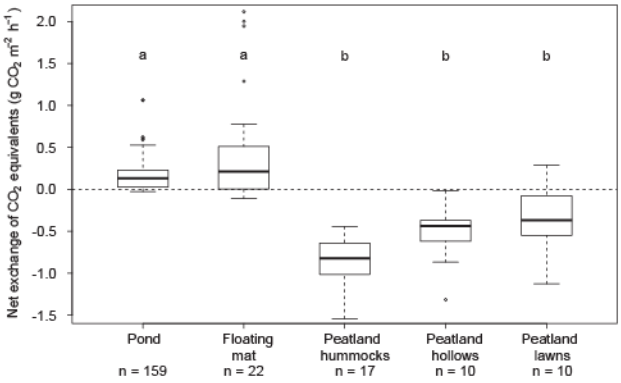

Figure 9. Daytime net exchange of CO_2 equivalents of the pond, the floating mat and the three different microforms of the peatland. Different letters indicate significant differences (Kruskal–Wallis multiple comparison test, $p < 0.001$, $n = 218$). For comparability of the CO_2 fluxes of the floating mat and the peatland, only maximum net ecosystem exchange at values of photosynthetically active radiation > 1000 µmol m^{-2} s^{-1} was used for the calculation. The bold horizontal line shows the median, the bottom and the top of the box the 25th and 75th percentile and the whiskers include all values within 1.5 times the interquartile range.

4 Discussion

4.1 Spatial pattern of CH_4 and CO_2 fluxes along the peatland – pond ecotone

The peatland and especially the floating mat were summer hot spots of CH_4 emissions compared to a variety of sites in other northern peatlands. Fluxes exceeded most, but not all, emissions reported by Hamilton et al. (1994), Strack et al. (2006), Dinsmore et al. (2009), Moore et al. (2011), and Trudeau et al. (2013) from similar environments by an order of magnitude (see also Supplement for a compilation of flux values, Tables S4–S6). On a per-day and mass basis mean fluxes reached 204 and 437 mg CH_4-C m^{-2} d^{-1}, which is at the high end of fluxes reported in meta-analyses (Olefeldt et al., 2013). Average CH_4 emissions from the open water were still substantial at 63 mg CH_4-C m^{-2} d^{-1}, which is about 5 times the flux reported from the multi-year study of Stordalen Mire in northern Sweden (Wik et al., 2013). Emissions fell, however, well into the range of fluxes reported from other peatland ponds (Huttunen et al., 2002; Trudeau et al., 2013; Pelletier et al., 2014). In contrast, CO_2 fluxes were fairly inconspicuous compared to fluxes in similar systems; on a per-day and mass basis mean maximum NEE reached −5.4 g CO_2-C m^{-2} d^{-1} in the bog and −1.27 g CO_2-C m^{-2} d^{-1} on the floating mat, and daytime ER 3.91 g CO_2-C m^{-2} d^{-1} and 1.85 g CO_2-C m^{-2} d^{-1}, respectively. The pond on average emitted 0.38 g CO_2-C m^{-2} d^{-1}. Both pond and floating mat thus lost more CO_2 than they fixed during the day, which suggests that in both environ-

ments additional CO_2 was released, for example stemming from carbon-rich groundwater seeping into the pond.

Part of the surprising source strength of methane can be attributed to the inclusion of ebullition by means of high frequency chamber measurements, similarly as first reported by Goodrich et al. (2011). Fluxes that are visibly affected by ebullition events have often been discarded from static chamber fluxes in the past because the non-linearity of concentration increase over time is problematic when few samples are analyzed by gas chromatography. Ebullition contributed on average 66 % to the emissions on the floating mat and reached 78 % at the plot with the highest methane flux (Figs. 4 and 7). The importance and variability of ebullition was similar as reported from an ombrotrophic peatland in Japan (50 to 64 %; Tokida et al., 2007). The CH_4 released by individual bubble events from the floating mat was also on the same order of magnitude as bubble CH_4 release in Sallie's Fen (Goodrich et al., 2011). At that site the bubble frequency of 35 ± 16 events $m^{-2}\,h^{-1}$ was, however, lower than on the floating mat at Wylde Lake Bog with 54 to 168 events $m^{-2}\,h^{-1}$. In contrast to these findings, ebullition accounted on average only for 20 % of fluxes at our bog site and 27 % in the pond (Figs. 3 and 5), where bubble frequency of outer plots was less than 9 events $m^{-2}\,h^{-1}$ and dropped to zero by the end of September (Fig. 3). In the pond ebullition was thus less important than reported previously in 11 lakes in Wisconsin (40 to 60 %; Bastviken et al., 2004) and two productive, urban ponds in Sweden and China (> 90 %; Natchimuthu et al., 2014; Xiao et al., 2014).

Even though bubbles were rarely observed on p1, p2 and p3 farther away from the floating mat (Fig. 7) and ceased altogether in September (Fig. 3), formation of CH_4 bubbles may have initially been possible in the pond sediments. Concentrations exceeded the threshold concentration of bubble formation at a N_2 partial pressure of 0.8 atm in all locations sampled (Fig. 6). Such concentrations were only reached at larger sediment depth, though, and ongoing stripping of N_2 with ebullition may have raised concentration thresholds over time (Fechner-Levy and Hemond, 1996). At a remaining N_2 partial pressure of 0.5 atm, ebullition was not possible from a theoretical point of view, which may explain its limited importance in the pond. The lack of ebullition later on may have been assisted by falling temperatures in autumn; a change from 20 to 10 °C, for example, raises the threshold for ebullition by 70 µmol L^{-1}. Flat or linearly increasing concentration profiles near the sediment–water interface (Fig. 6) also indicated a lack of active production of the gas in this zone. Concentrations of CH_4 and CO_2 remained low, typically less than 650 and 1500 µmol L^{-1}, respectively, suggesting that microbial activity in the sediments was limited. Also the diffusive fluxes were small in units of mass, about 3.5 mg CH_4-C $m^{-2}\,d^{-1}$ and 7.5 mg CO_2-C $m^{-2}\,d^{-1}$, respectively. The continuous emission of CH_4 and CO_2 from the pond, on average 63 mg CH_4-C $m^{-2}\,d^{-1}$ and 380 mg CO_2-C $m^{-2}\,d^{-1}$, was hence likely driven by respiration in the water column and by advective inflow of groundwater rich in CH_4 and CO_2.

Our results further suggest that medium and infrequent large bubble events contributed a substantial fraction to the total CH_4 flux at the floating mat but not in the bog and the pond (Fig. 8). This was the case even though small bubble events were much more frequent than large ones (Fig. 8). DelSontro et al. (2015) also reported a strong positive correlation between ebullition flux and bubble volume in open water and found that the largest 10 % of the bubbles observed in Lake Wohlen, Switzerland, accounted for 65 % of the CH_4 transport. According to the authors, large bubbles are disproportionately important because they contain exponentially more CH_4 with increasing diameter, rise faster, and have less time and a relatively smaller surface area to dissolve or exchange CH_4 with the surroundings (DelSontro et al., 2015).

The decline of CH_4 fluxes, CH_4 bubble frequency and contribution of ebullition from the floating mat to the open water was striking and fluxes were also considerably higher than at the peatland site (Fig. 7). These findings emphasize that the floating mats and transition zones to the open water need to be included when quantifying greenhouse gas budgets of pond and peatland ecosystems. We cannot mechanistically identify the causes for the observed pattern. It seems likely that the peak emissions from the floating mat were caused by an optimum of wet conditions in the peat, favoring methanogenesis and impeding methane oxidation, presence of some *Carex aquatilis* providing for conduit transport of the gas, and potentially by a release of methane from groundwater entering the land–water interface. CH_4 flux through plants with aerenchymatic tissues can be responsible for 50 to 97 % of the total CH_4 flux in peatlands because the aerenchyma link the anaerobic zone of CH_4 production with the atmosphere (Kelker and Chanton, 1997; Kutzbach et al., 2004; Shannon et al., 1996). Kutzbach et al. (2004) found a strong positive correlation between the density of *C. aquatilis* culms and CH_4 fluxes, as well as a contribution of 66 ± 20 % of the plant-mediated CH_4 flux through *C. aquatilis* to the total flux in wet polygonal tundra. Since ebullition dominated the CH_4 flux from the floating mat (Fig. 4) in our particular case this transport mechanism seemed to be of more limited importance, though. Also recently fixed substrates may have played a role for high CH_4 emissions from the floating mat. Several studies have found a positive correlation between the rate of photosynthesis and CH_4 emissions (Joabsson and Christensen, 2001; Ström et al., 2003), which has been explained by the quick allocation of assimilated labile carbon to the roots and subsequent exudation to the anaerobic rhizosphere (Dorodnikov et al., 2011). These recent photosynthates serve as a preferential source of CH_4 compared to older more recalcitrant organic matter (Chanton et al., 1995). Labile organic matter produced by vascular plants was probably also imported from the floating mat to the margin of the pond (Repo et al., 2007; Wik et al., 2013). Given the gradual

Table 1. Correlations of CH_4 and CO_2 fluxes of the pond with environmental variables. CH_4 flux comprises both ebullition and diffusion if not annotated otherwise.

Flux	Time period	Spearman's rho	*P*	*n*
Mean air temperature since sunrise				
CO_2	whole period	−0.54	< 0.001	147
CH_4	whole period	−0.36	< 0.001	147
Diffusive CH_4[a]	whole period	−0.67	< 0.001	119
Mean water temperature during measurements				
CO_2	whole period	−0.47	< 0.001	94
CH_4	whole period	−0.50	< 0.001	94
Diffusive CH_4[a]	whole period	−0.60	< 0.001	82
Mean PAR of the last 3 h				
CO_2	whole period	−0.49	< 0.001	147
Mean wind speed of the last 24 h				
CO_2	mid summer[b]	−0.35	< 0.05	43
CO_2	late summer[c]	+0.45	< 0.001	104
CO_2	whole period	not significant		
CH_4	mid summer[b]	−0.35	< 0.05	43
CH_4	late summer[c]	+0.63	< 0.001	104
CH_4	whole period	+0.26	< 0.01	147
Maximum wind speed of the last 24 h				
CO_2	mid summer[b]	−0.45	< 0.01	43
CO_2	late summer[c]	+0.35	< 0.001	104
CO_2	whole period	+0.17	< 0.05	147
CH_4	mid summer[b]	−0.55	< 0.001	43
CH_4	late summer[c]	+0.63	< 0.001	104
CH_4	whole period	+0.32	< 0.001	147

[a] only measurements without ebullition included, [b] 10 July to 7 August, [c] 15 August to 29 September.

Table 2. Correlations of CH_4 and CO_2 fluxes of the floating mat with environmental variables. CH_4 flux comprises both ebullition and diffusion if not annotated otherwise.

Flux	Time period	Spearman's rho	P	*n*
Mean air temperature since sunrise				
Max. NEE	whole period	+0.74	< 0.001	20
CH_4	whole period	−0.42	< 0.001	79
Mean mat temperature during measurements				
ER	whole period	−0.44	< 0.01	38
CH_4	whole period	−0.41	< 0.001	79
Diffusive CH_4[a]	whole period	−0.52	< 0.001	53
Mean PAR during measurements				
NEE	mid summer[b]	not significant		
NEE	late summer[c]	−0.60	< 0.01	26
NEE	whole period	−0.37	< 0.05	42

[a] only measurements without ebullition included, [b] 10 July to 7 August, [c] 15 August to 29 September.

decline of CH_4 fluxes along the transect CH_4-rich groundwater may also have entered the floating mat and the pond, a process that we did not investigate.

4.2 Controls on CH_4 and CO_2 fluxes

In agreement with earlier work air pressure change influenced methane flux. We observed 1.5- to 3-fold higher CH_4 fluxes from the floating mat and the pond during periods of decreasing compared to increasing air pressure (Fig. S4), which was very likely caused by increased ebullition (Wik et al., 2013). Decreased atmospheric pressure results in bubble expansion, which enhances buoyancy force and entails bubble rise (Chen and Slater, 2015).

The negative correlation of water and mat temperature with CH_4 and CO_2 fluxes from the pond and CH_4 flux and ER of the floating mat (Tables 1 and 2) was unexpected, as it is consensus that temperature is an important positive control on these fluxes (Pelletier et al., 2014; Roulet et al., 1997; Sachs et al., 2010; Wik et al., 2014). Also the potential effect of wind speed on CH_4 and CO_2 fluxes from the pond was ambiguous. Increasing wind speeds should stimulate the exchange of dissolved gases by increasing turbulence of both air and water close to the interface (Crusius and Wanninkhof, 2003). Before 15 August wind speed and CH_4 and CO_2 efflux from the pond were, however, negatively correlated, whereas the correlation was positive thereafter despite quite consistent wind speed patterns and surface water CO_2 concentrations throughout the whole study period (Figs. 2 and S2).

Both phenomena may be explained by internal biological processes, i.e., the growth and decay of a dense algal mat on the pond, changing hydrological connection between the pond system and the surrounding peatland, and the influence of the vascular vegetation on the floating mat. The algal mat developed in the beginning of July and was largely irreversibly dissolved by a storm on 12 August (Figs. S5 and S6). During its presence CO_2 emissions from the pond remained low (Fig. 3) and were overestimated by the boundary layer equation approach. Amplitudes of dissolved CO_2 concentration were strong and concentration decreased with increasing PAR (Table 1). Such dynamics reflects a strong autochthonous photosynthetic and respiratory activity and lack of water mixing. The empirical relationship between CO_2 concentration gradient, wind speed and flux, which is largely controlled by turbulence in the water column, obviously did not apply under such conditions. The subsequent shift to high CO_2 and CH_4 emissions was probably partly caused by the decomposition of the remains of the algal mat, similarly as reported from a boreal and a subtropical pond (Hamilton et al., 1994; Xiao et al., 2014). Other than that, the algal mat probably represented a physical barrier to diffusive and ebullitive gas exchange between water column and atmosphere. We observed trapped gas bubbles within the algal mat with CH_4 concentration of only 4 to 8 %; part of the originally contained CH_4 may have been re-dissolved and oxidized. Even in shallow lakes and ponds, CO_2 and CH_4 concentra-

tions can be several-fold higher in the deep water compared to the surface water during certain periods (Dinsmore et al., 2009; Ford et al., 2002). We can only assume that such concentration gradients established in or under the algal mat. Its destruction, mixing of the water column and resuspension of the upper sediment layer probably entailed the observed peak diffusive CO_2 and CH_4 emissions after the storm on 12 August (Figs. 2, 3).

4.3 Relevance of greenhouse gas emissions from the pond system

In terms of radiative forcing, the floating mat and open water behaved differently than the peatland site during our daytime flux measurements at $PAR > 1000\,\mu mol\,m^{-2}\,s^{-1}$. All three bog micro-sites represented daytime sinks of CO_2 equivalents and most so the hummocks (Fig. 9), which represented about 90 % of the area. The floating mat and to a lesser extent also the pond were sources of CO_2 equivalents to the atmosphere, even at daytime, and had a comparable source strength as the boreal ponds and beaver pond investigated by Hamilton et al. (1994) and Roulet et al. (1997). Net photosynthetic CO_2 uptake at light saturation was thus unable to counterbalance the high CH_4 emissions of the floating mat in terms of CO_2 equivalents; at both the floating mat and the pond emission of CH_4 was more important than CO_2 exchange in terms of greenhouse gas equivalents. In the pond the average contribution of CH_4 was 59 %, which is much higher than reported from a beaver pond at the Mer Bleue bog (5 %; Dinsmore et al., 2009), but comparable to figures from ponds in other studies (36 to 91 %; Hamilton et al., 1994; Huttunen et al., 2002; Pelletier et al., 2014; Repo et al., 2007; Roulet et al., 1997). We ascribe the large differences between the floating mat and the peatland site (Figs. 7 and 10) to the influx of allochthonous organic and inorganic carbon to the pond system from the surroundings and to the different vegetation composition, in particular the occurrence of *Carex aquatilis* on the floating mat, which may have enhanced CH_4 production and transport (Kutzbach et al., 2004; Strack et al., 2006). Our results support earlier suggestions that ponds are important for the greenhouse gas budget of peatlands at landscape scale (e.g., Pelletier et al., 2014) and they suggest that changes in the area extent of floating mats and shore length will be an important factor of changes in greenhouse gas budgets with predicted climate change.

5 Conclusions

Our summer measurements of atmospheric CH_4 and CO_2 exchange revealed a substantial small-scale spatial variability with 6- and 42-fold increasing median CH_4 fluxes and bubble frequencies, respectively, from the open water of the pond towards the surrounding floating mat. Individual bubble events releasing more than 10 µmol CH_4 contributed substantially to summer CH_4 emissions from the floating mat, despite their rare occurrence. When CH_4 emissions of peatlands that contain ponds are quantified, ebullitive and diffusive CH_4 fluxes at the land–water interface hence need to be accounted for and the areal cover of the different microforms and/or plant communities should be thoroughly mapped, as suggested by Sachs et al. (2010) for tundra landscape. We also observed 4- to 16-fold increases in CH_4 and CO_2 emissions in late summer that were unrelated to meteorological drivers, such as temperature, wind speed and radiation. Hydrological connections to adjacent peatlands and internal hydrological and biological processes, such as the development of algal mats, which can be abundant in small and shallow water bodies (e.g., Dinsmore et al., 2009; Hamilton et al., 1994; Xiao et al., 2014) thus require more attention in the future. During our summer daytime flux measurements, the pond system had a warming effect considering CH_4 and CO_2 exchange, with the highest net release of CO_2 equivalents from the floating mat. We conclude that carbon cycling and hydrology of small ponds and their surrounding ecotone need to be further investigated; these systems are hot spots of greenhouse gas exchange and are likely highly sensitive to anthropogenic climate change due to their shallowness and dependence on water budgets and hydrological processes upstream.

6 Data availability

The data published in this contribution can be accessed by email request to the corresponding author.

The Supplement related to this article is available online at doi:10.5194/bg-13-3777-2016-supplement.

Acknowledgements. The study was financially supported by the German Research Foundation (DFG) grant BL 563/21-1 and an international cooperation grant by the German Academic Exchange Service (DAAD) to C. Blodau. We thank C. Wagner-Riddle for the possibility to use the former Blodau laboratory at the School of Environmental Sciences at the University of Guelph and P. Smith and L. Wing for organizational and technical support. We are grateful to M. Neumann from the Grand River Conservation Authority for permission to conduct research in the Luther Marsh Wildlife Management Area, Ontario, Canada, Z. Green for kindly providing satellite images of the study area and C. A. Lacroix (OAC Herbarium, Biodiversity Institute of Ontario) for her friendly help in identifying some plants. We are thankful to M. Goebel for support in the field and advices on study design and data analysis and to E. Fleischer for her helpful comments.

Edited by: G. Wohlfahrt

References

Bastviken, D., Cole, J. J., Pace, M. L., and Tranvik, L. J.: Methane emissions from lakes: Dependence of lake characteristics, two regional assessments, and a global estimate, Global Biogeochem. Cy., 18, GB4009, doi:10.1029/2004GB002238, 2004.

Bastviken, D., Tranvik, L. J., Downing, J. A., Crill, P. M., and Enrich-Prast, A.: Freshwater Methane Emissions Offset the Continental Carbon Sink, Science, 331, p. 50, doi:10.1126/science.1196808, 2011.

Bridgham, S. D., Cadillo-Quiroz, H., Keller, J. K., and Zhuang, Q.: Methane emissions from wetlands: biogeochemical, microbial, and modeling perspectives from local to global scales, Glob. Change Biol., 19, 1325–1346, 2013.

Carmichael, M. J., Bernhardt, E. S., Bräuer, S. L., and Smith, W. K.: The role of vegetation in methane flux to the atmosphere: should vegetation be included as a distinct category in the global methane budget?, Biogeochemistry, 119, 1–24, 2014.

Chen, X. and Slater, L.: Gas bubble transport and emissions for shallow peat from a northern peatland: The role of pressure changes and peat structure, Water Resour. Res., 51, 151–168, 2015.

Ciais, P., Sabine, C., Bala, G., Bopp, L., Brovkin, V., Canadell, J., Chhabra, A., DeFries, R., Galloway, J., Heimann, M., Jones, C., Le Quéré, C., Myneni, R. B., Piao, S., and Thornton, P.: Carbon and Other Biogeochemical Cycles, in: Climate Change 2013: The Physical Science Basis, Contribution of Working Group I to the Fifth Assessment Report of the Intergovernmental Panel on Climate Change, edited by: Stocker, T. F., Qin, D., Plattner, G.-K., Tignor, M., Allen, S. K., Boschung, J., Nauels, A., Xia, Y., Bex, V., and Midgley, P. M., Cambridge, New York, 465–570, 2013.

Chanton, J. P., Bauer, J. E., Glaser, P. A., Siegel, D. I., Kelley, C. A., Tyler, S. C., Romanowicz, E. H., and Lazrus, A.: Radiocarbon evidence for the substrates supporting methane formation within northern Minnesota peatlands, Geochim. Cosmochim. Ac., 59, 3663–3668, 1995.

Cole, J. J., Prairie, Y. T., Caraco, N. F., McDowell, W. H., Tranvik, L. J., Striegl, R. G., Duarte, C. M., Kortelainen, P., Downing, J. A., Middelburg, J. J., and Melack, J.: Plumbing the global carbon cycle: Integrating inland waters into the terrestrial carbon budget, Ecosystems, 10, 171–184, 2007.

Crusius, J. and Wanninkhof, R.: Gas transfer velocities measured at low wind speed over a lake, Limnol. Oceanogr., 48, 1010–1017, 2003.

Davidson, E. A., Savage, K., Verchot, L. V., and Navarro, R.: Minimizing artifacts and biases in chamber-based measurements of soil respiration. Agr. Forest Meteorol., 113, 21–37, 2002.

DelSontro, T., McGinnis, D. F., Wehrli, B., and Ostrovsky, I.: Size Does Matter: Importance of Large Bubbles and Small-Scale Hot Spots for Methane Transport, Environ. Sci. Technol., 49, 1268–1276, 2015.

Dinsmore, K. J., Billett, M. F., and Moore, T. R.: Transfer of carbon dioxide and methane through the soil-water-atmosphere system at Mer Bleue peatland, Canada, Hydrol. Process., 23, 330–341, 2009.

Dinsmore, K. J., Billett, M. F., Skiba, U. M., Rees, R. M., Drewer, J., and Helfter, C.: Role of the aquatic pathway in the carbon and greenhouse gas budgets of a peatland catchment, Glob. Change Biol., 16, 2750–2762, 2010.

Dorodnikov, M., Knorr, K.-H., Kuzyakov, Y., and Wilmking, M.: Plant-mediated CH_4 transport and contribution of photosynthates to methanogenesis at a boreal mire: a ^{14}C pulse-labeling study, Biogeosciences, 8, 2365–2375, doi:10.5194/bg-8-2365-2011, 2011.

Downing, J. A.: Emerging global role of small lakes and ponds: little things mean a lot, Limnetica, 29, 9–24, 2010.

Downing, J. A., Cole, J. J., Middelburg, J. J., Striegl, R. G., Duarte, C. M., Kortelainen, P., Prairie, Y. T., and Laube, K. A.: Sediment organic carbon burial in agriculturally eutrophic impoundments over the last century, Global Biogeochem. Cy., 22, GB1018, doi:10.1029/2006GB002854, 2008.

Drösler, M.: Trace gas exchange and climatic relevance of bog ecosystems, Southern Germany, Doctoral thesis, Technical University of Munich, Munich, 2005.

Estop-Aragonés, C., Knorr, K. H., and Blodau, C.: Controls on in situ oxygen and DIC dynamics in peats of a temperate fen, J. Geophys. Res., 117, G02002, doi:10.1029/2011JG001888, 2012.

Fechner-Levy, E. J. and Hemond, H. F.: Trapped methane volume and potential effects on methane ebullition in a northern peatland, Limnol. Oceanogr., 41, 1375–1383, 1996.

Flessa, H., Rodionov, A., Guggenberger, G., Fuchs, H., Magdon, P., Shibistova, O., Zrazhevskaya, G., Mikheyeva, N., Kasansky, O., and Blodau, C.: Landscape controls of CH_4 fluxes in a catchment of the forest tundra ecotone in northern Siberia, Glob. Change Biol., 14, 2040–2056, 2008.

Ford, P. W., Boon, P. I., and Lee, K.: Methane and oxygen dynamics in a shallow floodplain lake: the significance of periodic stratification, Hydrobiologia, 485, 97–110, 2002.

Givelet, N., Roos-Barraclough, F., and Shotyk, W.: Predominant anthropogenic sources and rates of atmospheric mercury accumulation in southern Ontario recorded by peat cores from three bogs: comparison with natural "background" values (past 8000 years), J. Environ. Monitor., 5, 935–949, 2003.

Goodrich, J. P., Varner, R. K., Frolking, S., Duncan, B. N., and Crill, P. M.: High-frequency measurements of methane ebullition over a growing season at a temperate peatland site, Geophys. Res. Lett., 38, L07404, doi:10.1029/2011GL046915, 2011.

Grand River Conservation Authority: Orthoimagery, https://maps.grandriver.ca/maps-home.html (last access: 10 August 2015), Cambrige, Ontario, 2015.

Hamilton, J. D., Kelly, C. A., Rudd, J. W. M., Hesslein, R. H., and Roulet, N. T.: Flux to the atmosphere of CH_4 and CO_2 from wetland ponds on the Hudson Bay lowlands (HBLs), J. Geophys. Res., 99, 1495–1510, 1994.

Hesslein, R. H.: An in situ sampler for close interval pore water studies, Limnol. Oceanogr., 21, 912–914, 1976.

Huttunen, J. T., Väisänen, T. S., Heikkinen, M., Hellsten, S., Nykänen, H., Nenonen, O., and Martikainen, P. J.: Exchange of CO_2, CH_4 and N_2O between the atmosphere and two northern boreal ponds with catchments dominated by peatlands or forests, Plant Soil, 242, 137–146, 2002.

Joabsson, A. and Christensen, T. R.: Methane emissions from wetlands and their relationship with vascular plants: an Arctic example, Glob. Change Biol., 7, 919–932, 2001.

Juutinen, S., Alm, J., Martikainen, P., and Silvola, J.: Effects of spring flood and water level draw-down on methane dynamics in the littoral zone of boreal lakes, Freshwater Biol. 46, 855–869, 2001.

Juutinen, S., Rantakari, M., Kortelainen, P., Huttunen, J. T., Larmola, T., Alm, J., Silvola, J., and Martikainen, P. J.: Methane dynamics in different boreal lake types, Biogeosciences, 6, 209–223, doi:10.5194/bg-6-209-2009, 2009.

Juutinen, S., Väliranta, M., Kuutti, V., Laine, A. M., Virtanen, T., Seppä, H., Weckström, J., and Tuittila, E. S.: Short-term and long-term carbon dynamics in a northern peatland-stream-lake continuum: A catchment approach, J. Geophys. Res.-Biogeo., 118, 171–183, 2013.

Kelker, D. and Chanton, J.: The effect of clipping on methane emissions from *Carex*, Biogeochemistry, 39, 37–44, 1997.

Kelly, C. A., Fee, E., Ramlal, P. S., Rudd, J. W. M., Hesslein, R. H., Anema, C., and Schindler, E. U.: Natural variability of carbon dioxide and net epilimnetic production in the surface waters of boreal lakes of different sizes, Limnol. Oceanogr. 46, 1054–1064, 2001.

Kortelainen, P. L., Rantakari, M., Huttunen, J. T., Mattsson, T., Alm, J., Juutinen, S., Larmola, T., Silvola, J., and Martikainen, P. J.: Sediment respiration and lake trophic state are important predictors of large CO_2 evasion from small boreal lakes, Glob. Change Biol., 12, 1554–1567, 2006.

Kutzbach, L., Wagner, D., and Pfeiffer, E. M.: Effect of microrelief and vegetation on methane emission from wet polygonal tundra, Lena Delta, Northern Siberia, Biogeochemistry, 69, 341–362, 2004.

Larmola, T., Alm, J., Juutinen, S., Huttunen, J. T., Martikainen, P. J., and Silvola, J.: Contribution of vegetated littoral zone to winter fluxes of carbon dioxide and methane from boreal lakes, J. Geophys. Res.-Atmos., 109, D19102, doi:10.1029/2004JD004875, 2004.

Larmola, T., Bubier, J. L., Kobyljanec, C., Basiliko, N., Juutinen, S., Humphreys, E. R., Preston, M., and Moore, T. R.: Vegetation feedbacks of nutrient addition lead to a weaker carbon sink in an ombrotrophic bog, Glob. Change Biol., 19, 3729–3739, 2013.

Lerman, A.: Chemical exchange across sediment-water interface, Annu. Rev. Earth Pl. Sc., 6, 281–303, 1978.

Macrae, M. L., Bello, R. L., and Molot, L. A.: Long-term carbon storage and hydrological control of CO_2 exchange in tundra ponds in the Hudson Bay Lowland, Hydrol. Process., 18, 2051–2069, 2004.

McEnroe, N. A., Roulet, N. T., Moore, T. R., and Garneau, M.: Do pool surface area and depth control CO_2 and CH_4 fluxes from an ombrotrophic raised bog, James Bay, Canada?, J. Geophys. Res., 114, G01001, doi:10.1029/2007JG000639, 2009.

McLaughlin, J. and Webster, K.: Effects of Climate Change on Peatlands in the Far North of Ontario, Canada?: A Synthesis, Arct. Antarct. Alp. Res., 46, 84–102, 2014.

Moore, T. R., De Young, A., Bubier, J. L., Humphreys, E. R., Lafleur, P. M., and Roulet, N. T.: A Multi-Year Record of Methane Flux at the Mer Bleue Bog, Southern Canada, Ecosystems, 14, 646–657, 2011.

Michmerhuizen, C. M., Striegl, R. G., and McDonald, M. E.: Potential methane emission from north-temperate lakes following ice melt, Limnol. Oceanogr., 41, 985–991, 1996.

Myhre, G., Shindell, D., Bréon, F.-M., Collins, W., Fuglestvedt, J., Huang, J., Koch, D., Lamarque, J.-F., Lee, D., Mendoza, B., Nakajima, T., Robock, A., Stephens, G., Takemura, T., and Zhang, H.: Anthropogenic and Natural Radiative Forcing, in: Stocker, T. F., Qin, D., Plattner, G.-K., Tignor, M., Allen, S. K., Boschung, J., Nauels, A., Xia, Y., Bex, V., and Midgley, P. M., Climate Change 2013: The Physical Science Basis. Contribution of Working Group I to the Fifth Assessment Report of the Intergovernmental Panel on Climate Change, Cambridge, New York, 659–740, 2013.

Natchimuthu, S., Panneer Selvam, B., and Bastviken, D.: Influence of weather variables on methane and carbon dioxide flux from a shallow pond, Biogeochemistry, 119, 403–413, 2014.

National Climate Data and Information Archive: Canadian Climate Normals, http://climate.weather.gc.ca/climate_normals/index_e.html, last access: 18 November 2014.

Olefeldt, D., Turetsky, M. R., Crill, P. M., and McGuire, A. D.: Environmental and physical controls on northern terrestrial methane emissions across permafrost zones, Glob. Change Biol., 19, 589–603, 2013.

Pelletier, L., Strachan, I. B., Garneau, M., and Roulet, N. T.: Carbon release from boreal peatland open water pools: Implication for the contemporary C exchange, J. Geophys. Res.-Biogeo., 119, 207–222, 2014.

Raymond, P. A., Hartmann, J., Lauerwald, R., Sobek, S., McDonald, C., Hoover, M., Butman, D., Striegl, R. G., Mayorga, E., Humborg, C., Kortelainen, P. L., Dürr, H., Meybeck, M., Ciais, P., and Guth, P.: Global carbon dioxide emissions from inland waters, Nature, 503, 355–359, 2013.

R Core Team: R: A language and environment for statistical computing, R Foundation for Statistical Computing, Vienna, 2014.

Repo, M. E., Huttunen, J. T., Naumov, A. V., Chichulin, A. V., Lapshina, E. D., Bleuten, W., and Martikainen, P. J.: Release of CO_2 and CH_4 from small wetland lakes in western Siberia, Tellus, 59B, 788–796, 2007.

Roulet, N. T., Crill, P. M., Comer, N. T., Dove, A., and Boubonniere, R. A.: Flux between a boreal beaver pond and the atmosphere, J. Geophys. Res., 102, 29313–29319, 1997.

Sachs, T., Giebels, M., Boike, J., and Kutzbach, L.: Environmental controls on CH_4 emission from polygonal tundra on the microsite scale in the Lena river delta, Siberia, Glob. Change Biol., 16, 3096–3110, 2010.

Sander, R.: Compilation of Henry's Law Constants for Inorganic and Organic Species of Potential Importance in Environmental Chemistry, Max-Planck Institute of Chemistry, Mainz, 1999.

Sandilands, A. P.: Annotated Checklist of the Vascular Plants and Vertebrates of Luther Marsh, Ontario, Ontario Field Biologist, Special Publication No. 2. 1984.

Shannon, R. D., White, J. R., Lawson, J. E., and Gilmour, B. S.: Methane efflux from emergent vegetation in peatlands, J. Ecol., 84, 239–246, 1996.

Soumis, N., Canuel, R., and Lucotte, M.: Evaluation of two current approaches for the measurement of carbon dioxide diffusive fluxes from lentic ecosystems, Environ. Sci. Technol., 42, 2964–2969, 2008.

Strack, M., Waller, M. F., and Waddington, J. M.: Sedge succession and peatland methane dynamics: A potential feedback to climate change, Ecosystems, 9, 278–287, 2006.

Ström, L., Ekberg, A., Mastepanov, M., and Christensen, T. R.: The effect of vascular plants on carbon turnover and methane emissions from a tundra wetland, Glob. Change Biol., 9, 1185–1192, 2003.

Sugimoto, A. and Fujita, N.: Characteristics of methane emissions from different vegetations on a wetland, Tellus, 49B, 382–392, 1997.

Tokida, T., Miyazaki, T., Mizoguchi, M., Nagata, O., Takakai, F., Kagemoto, A., and Hatano, R.: Falling atmospheric pressure as a trigger for methane ebullition from peatland, Global Biogeochem. Cy., 21, GB2003, doi:10.1029/2006GB002790, 2007.

Tranvik, L. J., Downing, J. A., Cotner, J. B., Loiselle, S. A., Striegl, R. G., Ballatore, T. J., Dillon, P., Finlay, K., Fortino, K., Knoll, L. B., Kortelainen, P. L., Kutser, T., Larsen, S., Laurion, I., Leech, D. M., McCallister, S. L., Mcknight, D. M., Melack, J. M., Overholt, E., Porter, J. A., Prairie, Y. T., Renwick, W. H., Roland, F., Sherman, B. S., Schindler, D. W., Sobek, S., Tremblay, A., Vanni, M. J., Verschoor, A. M., Von Wachenfeldt, E., and Weyhenmeyer, G. A.: Lakes and reservoirs as regulators of carbon cycling and climate, Limnol. Oceanogr., 54, 2298–2314, 2009.

Trudeau, N. C., Garneau, M., and Pelletier, L.: Methane fluxes from a patterned fen of the northeastern part of the La Grande river watershed, James Bay, Canada, Biogeochemistry, 113, 409–422, 2013.

Turunen, J., Tomppo, E., Tolonen, K., and Reinikainen, A.: Estimating carbon accumulation rates of undrained mires in Finland – application to boreal and subarctic regions, The Holocene, 12, 69–80, 2002.

Varadharajan, C. and Hemond, H. F.: Time-series analysis of high-resolution ebullition fluxes from a stratified, freshwater lake, J. Geophys. Res.-Biogeo., 117, G02004, doi:10.1029/2011JG001866, 2012.

Verpoorter, C., Kutser, T., Seekell, D. A., and Tranvik, L. J.: A global inventory of lakes based on high-resolution satellite imagery, Geophys. Res. Lett., 41, 6396–6402, 2014.

Walter, K. M., Zimov, S. A., Chanton, J. P., Verbyla, D., and Chapin, F. S.: Methane bubbling from Siberian thaw lakes as a positive feedback to climate warming, Nature, 443, 71–75, 2006.

Wik, M., Crill, P. M., Varner, R. K., and Bastviken, D.: Multiyear measurements of ebullitive methane flux from three subarctic lakes, J. Geophys. Res.-Biogeo., 118, 1307–1321, 2013.

Wik, M., Thornton, B. F., Bastviken, D., MacIntyre, S., Varner, R. K., and Crill, P. M.: Energy input is primary controller of methane bubbling in subarctic lakes, Geophys. Res. Lett., 41, 555–560, 2014.

Xenopoulos, M. A., Lodge, D. M., Frentress, J., Kreps, T. A., Bridgham, S. D., Grossman, E., and Jackson, C. J.: Regional comparisons of watershed determinants of dissolved organic carbon in temperate lakes from the Upper Great Lakes region and selected regions globally, Limnol. Oceanogr., 48, 2321–2334, 2003.

Xiao, S., Yang, H., Liu, D., Zhang, C., Lei, D., Wang, Y., Peng, F., Li, Y., Wang, C., Li, X., Wu, G., and Liu, L.: Gas transfer velocities of methane and carbon dioxide in a subtropical shallow pond, Tellus, 66B, 23795, doi:10.3402/tellusb.v67.27480, 2014.